

Nuclear Radii from Nuclear Masses

O. A. P. Tavares and E. L. Medeiros¹

Centro Brasileiro de Pesquisas Físicas - CBPF/MCTIC

Rua Dr. Xavier Sigaud 150, 22290-180 Rio de Janeiro-RJ, Brazil

*Dedicated to CBPF - Centro Brasileiro de Pesquisas Físicas on the occasion of
the 70th anniversary of its foundation.*

Abstract - Single uncharged pion production in neutron- and proton-induced reactions on complex nuclei, combined with the nuclear Fermi Gas Model, has been used to evaluate the average equivalent radius of a (Z, A) nucleus directly from the experimental nuclear mass-values of (Z, A) and its neighbors $(Z, A-1)$ and $(Z-1, A-1)$ isobars. A simple formula without adjustable parameters has been derived which gives nuclear radius-values that are in good agreement with updated, equivalent rms radius-values derived from experiments for a set of 540 nuclides comprising spherical, quasi-spherical, stable and long-term half-life nuclides. We shall call by RFNM-approach the present method of nuclear radius determination.

Keywords: average equivalent nuclear radii • nuclear masses • np and pn \rightarrow $d\pi^0$ reactions
• nuclear Fermi gas model • spherical and quasi-spherical nuclei • stable and long-lived nuclides

PACS: 21.10.Dr, 21.60.-n, 21.90.+f, 25.40.Ep, 25.40.Fq

¹Corresponding-author e-mail: emil@cbpf.br

1 Introduction

The present paper reports on the development and applications of an alternative method of estimating of the average radius-value, Q_A , of any nucleus (Z, A) of atomic number Z and mass number A . The approach to radius determination described below has been developed according to two basic ideas. The first one is to consider single uncharged pion production nuclear reactions induced by protons and neutrons, for which reactions it has been supposed that the threshold kinetic energy of the incident particle should be the same as in the head-on primary collisions $np \rightarrow d\pi^0$ and $pn \rightarrow d\pi^0$ that take place at the boundaries of the nuclear surface.

In second place, it has been considered the target Z protons and $A - Z$ neutrons moving like in separated Fermi gases of protons and neutrons, where their respective average kinetic energies are those occurring in the head-on collisions mentioned above.

These two hypotheses lead to a simple, direct dependence between the nuclear radius of (Z, A) , Q_A , and the nuclear masses of its neighbor $(Z, A - 1)$ and $(Z - 1, A - 1)$ isobars. Since the Fermi gases of protons and neutrons are independent of each other, there will be a value for the radius of the spherical volume that contains the Z protons, R_p , and another one where the $A - Z$ neutrons are contained, R_n .

The weighted average $Q_A = (Z/A) \cdot R_p + (1 - Z/A) \cdot R_n$ will represent the final value for the estimated radius of the (Z, A) nucleus. The radial extent of the atomic nucleus, in this way, is dictated by the extreme point at the nuclear surface where the thresholds of the primary reactions $np \rightarrow d\pi^0$ and $pn \rightarrow d\pi^0$ are just the same as for the respective nuclear reactions of $d\pi^0$ production from the complex (Z, A) nucleus. It should be pointed out that these single π^0 production reactions exhibit the lowest threshold energy-value (275 MeV) among all the fourteen primary single pion production reactions, and, in addition, uncharged pions have a mean lifetime of the order of 10^{-16} s.

The authors anticipate that the calculated average nuclear radius-values, Q_A , following the approach outlined above compare well with hundreds of experimental, equivalent root-mean-squares charge radii extracted from the updated compilation of radius-data reported by Angeli and Marinova [1].

2 A simple model to evaluate nuclear size

Let us consider the target nucleus (Z, A) of mass M_T at rest, and the two possible reactions of π^0 production induced by a neutron or proton leading to production of a deuteron and the residual nucleus (Z', A') of rest mass M_R . These reactions occur through the primary interactions

$$p + n \rightarrow d + \pi^0 \quad \text{and} \quad n + p \rightarrow d + \pi^0, \quad (1)$$

i.e.,

$$p + (Z, A) \rightarrow (Z, A - 1) + d + \pi^0, \quad (2)$$

when the target nucleon is a neutron, and

$$n + (Z, A) \rightarrow (Z - 1, A - 1) + d + \pi^0, \quad (3)$$

when the target nucleon is a proton. By expressing masses in u (atomic mass unit), the threshold kinetic energy of the projectile (proton or neutron), T_P^{th} , for reactions (2) and (3) are obtained by

$$T_P^{\text{th}} = \frac{F}{2M_T} [(m_d + m_{\pi^0} + M_R)^2 - (m_P + M_T)^2] \text{ MeV}, \quad (4)$$

where $F = 931.4940038$ MeV/u is the mass-energy conversion constant, $m_d = 2.013553213$ u is the deuteron rest mass, $m_{\pi^0} = 0.14490334$ u is the π^0 rest mass, and m_P denotes the projectile rest mass ($m_n = 1.0086649158$ u for neutron, and $m_p = 1.00727646693$ u for proton).

Nuclear mass-values for the target (M_T) and residual (M_R) nuclei to be used in (4) have been obtained by the usual way, *viz.*,

$$M = A - Zm_e + \frac{\Delta M + kZ^\beta}{F}, \quad (5)$$

in which $m_e = 0.548579909 \times 10^{-3}$ u is the electron rest mass, and ΔM is the atomic mass-excess, the values of which (expressed in MeV) have been taken from the AME2016 [2]. The quantity kZ^β represents the total binding energy of the Z electrons in the atom, where the constants k and β take the values

$$\begin{aligned} k &= 13.6 \times 10^{-6} \text{ MeV} \quad \text{and} \quad \beta = 2.408 \quad \text{for} \quad Z < 60, \\ \text{and} \quad k &= 8.7 \times 10^{-6} \text{ MeV} \quad \text{and} \quad \beta = 2.517 \quad \text{for} \quad Z \geq 60, \end{aligned} \quad (6)$$

as they come from data reported by Huang *et al.* [3].

The mechanism for pion production in reactions (2) and (3) consists of the primary interactions (1), where the target nucleon is moving at random inside the target nucleus. The projectile threshold kinetic energy, T_P^{th} , is then obtained from the head-on collisions that take place at the

nuclear boundary between the incident projectile and the target nucleon moving with average kinetic energy \overline{T}_t . This quantity will be derived subsequently by using the early Fermi Gas Model of the atomic nucleus. In such collisions the total energy in the CM system, E , must be equal to the sum of the rest masses of the primary reaction products, *i.e.*,

$$m_P^2 c^4 + m_t^2 c^4 + 2E_P E_t (1 - \beta_P \beta_t \cos \theta) = (m_d + m_{\pi^0})^2 c^4. \quad (7)$$

Here, subscript t identifies the quantities associated to the target nucleon, and $\theta = 180^\circ$. In addition,

$$E_P = T_P^{\text{th}} + m_P c^2, \quad E_t = \overline{T}_t + m_t c^2, \quad (8)$$

$$\beta_P = \left[1 - \left(\frac{T_P^{\text{th}}}{m_P c^2} + 1 \right)^{-2} \right]^{1/2}, \quad \beta_t = \left[1 - \left(\frac{\overline{T}_t}{m_t c^2} + 1 \right)^{-2} \right]^{1/2}.$$

By solving (7) for \overline{T}_t it gives

$$\overline{T}_t = F m_t x_t, \quad x_t = C (1 + q_t) - \left\{ 1 + [(C^2 - 1) q_t (q_t + 2)]^{\frac{1}{2}} \right\}, \quad (9)$$

where

$$q_t = \frac{(m_d + m_{\pi^0} + M_R)^2 - (m_P + M_T)^2}{2m_P M_T}, \quad t = n, p \quad (10)$$

$$\text{and } C = \frac{(m_d + m_{\pi^0})^2 - (m_P^2 + m_t^2)}{2m_P m_t} = 1.292771873.$$

Both q_t and C are dimensionless quantities, the former one being dependent on mass-values of the target and residual nuclei in the π^0 production reactions (2) and (3), and C is constant. Recall that $P = p$ when $t = n$, and $P = n$ when $t = p$.

The average kinetic energy of the target nucleon, \overline{T}_t , has been derived from the nuclear Fermi Gas Model. Accordingly, the distribution of the kinetic energy states of the target nucleons, T_t , in a Fermi gas of Z protons or $A - Z$ neutrons of a target nucleus (Z, A) in its ground state is given by

$$\frac{dn}{dT_t} = K \cdot T_t^{1/2}, \quad K = \frac{16\sqrt{2}\pi^2}{3} \cdot \frac{m_t^{3/2}}{h^3} \cdot R_i^3, \quad i = p, n \quad (11)$$

in which R_i represents the radius of the spherical volume which contains the Fermi gas of protons or neutrons, and $h = 6.626069574 \times 10^{-27}$ erg·s is Planck's constant. The average equivalent nuclear radius is then evaluated as

$$Q_A = \frac{Z}{A} \cdot R_p + \left(1 - \frac{Z}{A} \right) \cdot R_n. \quad (12)$$

To evaluate \overline{T}_t , let \mathcal{N} be the number of protons (Z) or neutrons ($A - Z$) contained in the spherical volumes of radii R_p and R_n , respectively. Since these particles are fermions, the energy

levels are filled with no more than two protons or two neutrons up to the Fermi energy, T_t^F , the highest energy level allowed for nucleons. So, the total number of energy levels, n_T , should be $n_T = \mathcal{N}/2$ for even \mathcal{N} , and $n_T = (\mathcal{N} + 1)/2$ for odd \mathcal{N} . Now, the energy interval $0 - T_t^F$ is divided into $n_T - 1$ equal intervals of width ΔT_t in such a way that $T_t^F = (n_T - 1) \cdot \Delta T_t$. The distribution (11) isn't strictly a continuous function for, even for heavy nuclei ($Z \approx 80 - 100$, $A - Z \approx 120 - 160$) the number of particles is relatively small, so that the integrals which appear to calculate the total number of energy levels, n_T , and the average energy level, \bar{T}_t , should be replaced by sums. Therefore, one has

$$n_T = K \cdot (\Delta T_t)^{3/2} \cdot S(n_T), \quad S(n_T) = 1 + 2^{1/2} + 3^{1/2} + \dots + (n_T - 1)^{1/2}, \quad (13)$$

and

$$\bar{T}_t = \frac{\Delta T_t \cdot S'(n_T)}{S(n_T)}, \quad S'(n_T) = 1 + 2^{3/2} + 3^{3/2} + \dots + (n_T - 1)^{3/2}. \quad (14)$$

By combining (13) and (14), it results

$$\bar{T}_t = \frac{G(n_T)}{K^{2/3}}, \quad G(n_T) = \frac{n_T^{2/3} \cdot S'(n_T)}{[S(n_T)]^{5/3}}. \quad (15)$$

$G(n_T)$ is a smooth, increasing, concave downward function (for nuclei of $A \geq 40$, $G(n_T)$ scales as $n_T^{2/3}$).

Introducing \bar{T}_t and K as they are given by (9) and (11), respectively, into (15), and expressing radii in fm, one obtains, finally,

$$R_p = 0.314123 \left(\frac{G_p(n_T)}{x_p} \right)^{1/2} \quad \text{and} \quad R_n = 0.313691 \left(\frac{G_n(n_T)}{x_n} \right)^{1/2}. \quad (16)$$

($G_p(n_T)$ and $G_n(n_T)$ refer, respectively, to the Fermi gas of Z protons and $A - Z$ neutrons). Since n_T depends only upon Z protons or $A - Z$ neutrons, and the quantity $x_{p,n}$ upon the nuclear masses of (Z, A) , $(Z, A - 1)$ and $(Z - 1, A - 1)$ nuclei through (9) and (10), it follows that the radius of the (Z, A) nucleus as calculated from (12) results directly from its nuclear mass-value and the ones of their neighbor $(Z, A - 1)$ and $(Z - 1, A - 1)$ isobars.

3 Results and discussion

Fig. 1 shows in part a) the calculated trends of the proton and neutron radii (R_p and R_n , respectively), and the average, equivalent nuclear radius (Q_A , eq. (12)) following the present RFNM-approach as a function of mass number, A , for a number of nuclei along and near the line of beta

stability. In fig. 1-b it is depicted the reduced radius, $Q_A/A^{1/3}$, for the same nuclei. For comparison, the equivalent root-mean-squares radius, $Q_e = \sqrt{5/3} \langle r^2 \rangle^{1/2}$ and its reduced form, $Q_e/A^{1/3}$, as deduced from the experimental rms radius-data reported by Angeli and Marinova [1] are also reported in parts a) and b), respectively. It is seen a very good similarity between the trends from the presently calculated radius-values and those coming from the experiments. The trends in fig. 1-b reveal a strong decrease of the reduced radius when one passes from less-massive nuclei ($A \approx 16-20$) to heavy ones ($A \geq 200$) (a reduction by $\sim 10-13\%$, thus reflecting a clear degree of nuclear compressibility, therefore, making the simple parametrization Q_A or Q_e proportional to $A^{1/3}$ not applicable equally to all nuclei.

It turns out that almost 60% of all stable plus long-lived nuclides selected to construct fig. 1 exhibit a significant degree of quadrupole deformation, $|\delta|$, like greater than $\sim 10\%$. Since the present method of radius determination has been developed under the assumption of spherical approximation for the atomic nucleus, it would be more appropriate to compare the presently calculated radii (eq. (12)) with the experimental, equivalent rms radii for all spherical and quasi-spherical nuclei, *i.e.*, those nuclei for which $|\delta| < 10\%$ that are listed in table 1 of Ref. [1].

The shape of the axially symmetric, ground state deformed nucleus is given by the quadrupole deformation parameter, β_2 , which is (to second order in β_2) connected to the intrinsic electric quadrupole moment, Q_2 , as [4]

$$Q_2 \approx \frac{3}{500} Z R_{\text{ch}}^2 \sqrt{\frac{5}{\pi}} \beta_2 \left[1 + \frac{2}{7} \sqrt{\frac{5}{\pi}} \beta_2 \right] \text{ barn}, \quad (17)$$

so that the quantity δ can be defined as

$$\delta = \frac{100 Q_2}{Z R_{\text{ch}}^2} \approx 0.7569 \beta_2 + 0.2728 \beta_2^2. \quad (18)$$

Therefore, it results that $|\delta| < 10\%$ when β_2 -values are found in the interval $-0.139 < \beta_2 < 0.127$. By searching for the most recent β_2 -values resulting from the Finite-Range-Droplet-Model (2012) of atomic nuclei as tabulated by Möller *et al.* [5], it has been possible to identify three-hundred and eighty-three spherical plus quasi-spherical nuclei of $|\delta| < 10\%$ in the compilation of the experimental data of Ref. [1]. In fig. 2 the differences $\Delta Q = Q_A - Q_e$, between the presently calculated average radii (eq. (12)) and the experimental ones $Q_e = \sqrt{5/3} \langle r^2 \rangle^{1/2}$ [1], have been plotted against mass number for all these spherical and quasi-spherical nuclei. Such ΔQ -values show to be distributed as a normal Gaussian curve around the mean value $\langle \Delta Q \rangle = -0.00567$ and standard deviation $\sigma = 0.08779$, with $\chi_\nu^2 = 1.2$. In about 70% of cases the values of Q_A and Q_e differ from each other by less than 1.5%.

The correlation between nuclear radii and nuclear masses is exemplified to some detail in figs. 3 and 4. Fig. 3 shows the case for the sequence of $^{202-214}\text{Pb}$ isotopes. Excess-mass values (fig. 3-a) and total electron binding energies (eqs. (5)–(6)) are used to obtain the quantities q_n and q_p (eq. (10)), and then they are inserted into eq. (9) to give the values of x_n and x_p (fig. 3-b). $x(q)$ is a smooth, concave upward function which decreases from $C - 1$ at $q = 0$ down to 0 at $q = C - 1$ (C is the constant given in (10)). The quantities x_n and x_p carry both the pairing and shell effects exhibited by nuclear masses, especially when neutrons are target nucleons. The resulting radii of the volumes of the Fermi gases of protons (R_p) and neutrons (R_n) reflect the structures showed by x_n and x_p (fig. 3-c), and the final value for the nuclear radius, Q_A , is obtained by weighted averaging R_p and R_n following eq. (12). Results so obtained compare well with the equivalent radius-values derived from experiments (differences in this sequence of lead isotopes have resulted to less than $\sim 1.3\%$).

Another example can be seen in fig. 4, where the various quantities that enter into radius determinations of $^{82-92}\text{Sr}$ isotopes have been plotted as a function of neutron number. Similarly to fig. 3, pairing and shell structures are seen for mass-excess, and x_n and x_p , as well as similar trends for the nuclear radii R_p , R_n and Q_A . Note that in both examples the maximum difference $Q_A - Q_e$ has resulted just at neutron-shell closures. This is partially due to the fact that the experimental Q_e -values in Ref. [1] come from the rms nuclear charge radii, being not considered the radii of the neutron distribution in nuclei. This issue will be treated in a future study on nuclear radius.

4 Conclusion

To conclude, we can say that the present RFNM-procedure for nuclear radii evaluation provides satisfactory results indeed, very close to the equivalent rms radius-values of the charge distribution for a great number of nuclei. The primary reactions of head-on collisions $np \rightarrow d\pi^0$ and $pn \rightarrow d\pi^0$ occurring at the boundaries of the atomic nuclei were able to provide good estimates for the average size (in the spherical approximation) for hundreds of nuclei. We believe that comparisons of the calculated radii by the present RFNM-approach with systematics of equivalent radii following the droplet model of atomic nuclei [6] with updated parameter-values [5], and the proton and neutron radii using the SLy4 parametrization of the Skirme-like force [7] will give much better agreement between each other data.

References

- [1] I. Angeli and K. P. Marinova, Table of experimental nuclear ground state charge radii: An update, *At. Data Nucl. Data Tables* **99** (2013) 69–95. <https://doi:10.1016/j.adt.2011.12.006>.
- [2] M. Wang, G. Audi, F. G. Kondev, W. J. Huang, S. Naimi and X. Xu, The AME2016 atomic mass evaluation (II) Tables, graphs and references, *Chin. Phys. C* **41** (2017) 030003.
- [3] K. -N. Huang, M. Aoyagi, M. H. Chen, B. Crasemann and H. Mark, Neutral-atom electron binding energies from relaxed-orbital relativistic Hartree-Fock-Slater calculations $2 \leq Z \leq 106$, *At. Data Nucl. Data Tables* **18** (1976) 243–291. [https://doi.org/10.1016/0092-640X\(76\)90027-9](https://doi.org/10.1016/0092-640X(76)90027-9).
- [4] K. E. G. Löbner, M. Vetter and V. Hönl, Nuclear Intrinsic Quadrupole Moments and Deformation Parameters, *At. Data Nucl. Data Tables* **7** (1970) 495–520. [https://doi.org/10.1016/S0092-640X\(18\)30059-7](https://doi.org/10.1016/S0092-640X(18)30059-7).
- [5] P. Möller, A. J. Sierk, T. Ichikawa and H. Sagawa, Nuclear ground-state masses and deformations: FRDM (2012), *At. Data Nucl. Data Tables* **109–110** (2016) 1–204. <https://doi.org/10.1016/j.adt.2015.10.002>.
- [6] W. D. Myers, Droplet model of atomic nuclei, IFI/Plenum, New York, 1977.
- [7] W. M. Seif and H. Mansour, Systematics of nucleon density distributions and neutron skin of nuclei, *Int. J. Mod. Phys. E* **24** (2015) 1550083. <https://doi.org/10.1142/S0218301315500834>.

Figure Captions

Fig. 1 Trends of the radial extent of atomic nuclei plotted against mass number, A , for the two-hundred and forty-seven stable plus thirty long-term half-life nuclides of Z and $N \geq 8$. In part a) the gray long-dashed lines labeled R_n and R_p correspond to calculated neutron and proton radii, respectively, following the present RFNM-approach (eq. (16)), and the gray full line is the trend of the average nuclear radius, Q_A , as obtained by eq. (12); points represent the experimental, equivalent rms charge radius, $Q_e = \sqrt{5/3} \langle r^2 \rangle^{1/2}$, of data taken from [1]; the inset shows the frequency distribution of the difference $\Delta Q = Q_A - Q_e$. Part b) shows the trend of the reduced radii $Q_A/A^{1/3}$ and $Q_e/A^{1/3}$, for the same nuclei. For the sake of clarity, only a few experimental data points have been plotted.

Fig. 2 The difference $\Delta Q = Q_A - Q_e$ between calculated and experimental radii is plotted *versus* mass number, A , for three-hundred and eighty-three spherical and quasi-spherical nuclei of degree of deformation $|\delta| < 10\%$ (see text for details). Q_A -values are those obtained according to the present RFNM-approach (eq. (12)), and Q_e -values are the experimental, equivalent rms charge radius-values given by $Q_e = \sqrt{5/3} \langle r^2 \rangle^{1/2}$, where $\langle r^2 \rangle^{1/2}$ charge radii are those tabulated in [1]. The regions of nuclei of neutron and proton shell-closures are indicated by arrows, and the distribution of the ΔQ -values is attached at right.

Fig. 3 Illustrating the direct correlation between the radius of a nucleus (Z, A) and the nuclear masses of (Z, A) and its neighbor ($Z, A - 1$) and ($Z - 1, A - 1$) isobars. It is shown the case for $^{202-214}\text{Pb}$ isotopes. In the inset scheme of part a), from right to left, a colliding proton with a target neutron of (Z, A) produces the residual ($Z, A - 1$), and from top to bottom, the collision of a neutron with a target proton of (Z, A) leads to residual ($Z - 1, A - 1$); the pair $d + \pi^0$ is formed in both reactions. Mass-excess of the lead and thallium isotopes that enter into the determination of the radius of (Z, A) nucleus are plotted *versus* neutron number, N ; note the change in slope at $N = 126$ shell closure. In part b), the quantity x defined by eq. (9) is plotted as full circles for the proton Fermi gas (x_p), and open circles for the neutron Fermi gas (x_n); pairing effect is clearly seen in both cases; for target neutrons the strong “saw-tooth” structure jumps by $\sim 5.6\%$ from $N = 126$ on. In part (c), the resulting radius-values R_n (open circles) and R_p (full circles) reflect the respective trends of x_n and x_p ; the final average nuclear radius, Q_A (open triangles, eq. (12)), compare well with the experimental, equivalent rms charge radius, Q_e (full squares [1]).

Fig. 4 The same as in fig. 3, but for $^{82-92}\text{Sr}$ isotopes. In this case, the minimum of ΔM occurs at $N = 50$ shell closure. Like in fig. 3, the “saw-tooth” structure in x_n jumps from $N = 50$

on. Only in two cases the final calculated Q_A -values differ from the experimental ones by more than 1.5%.

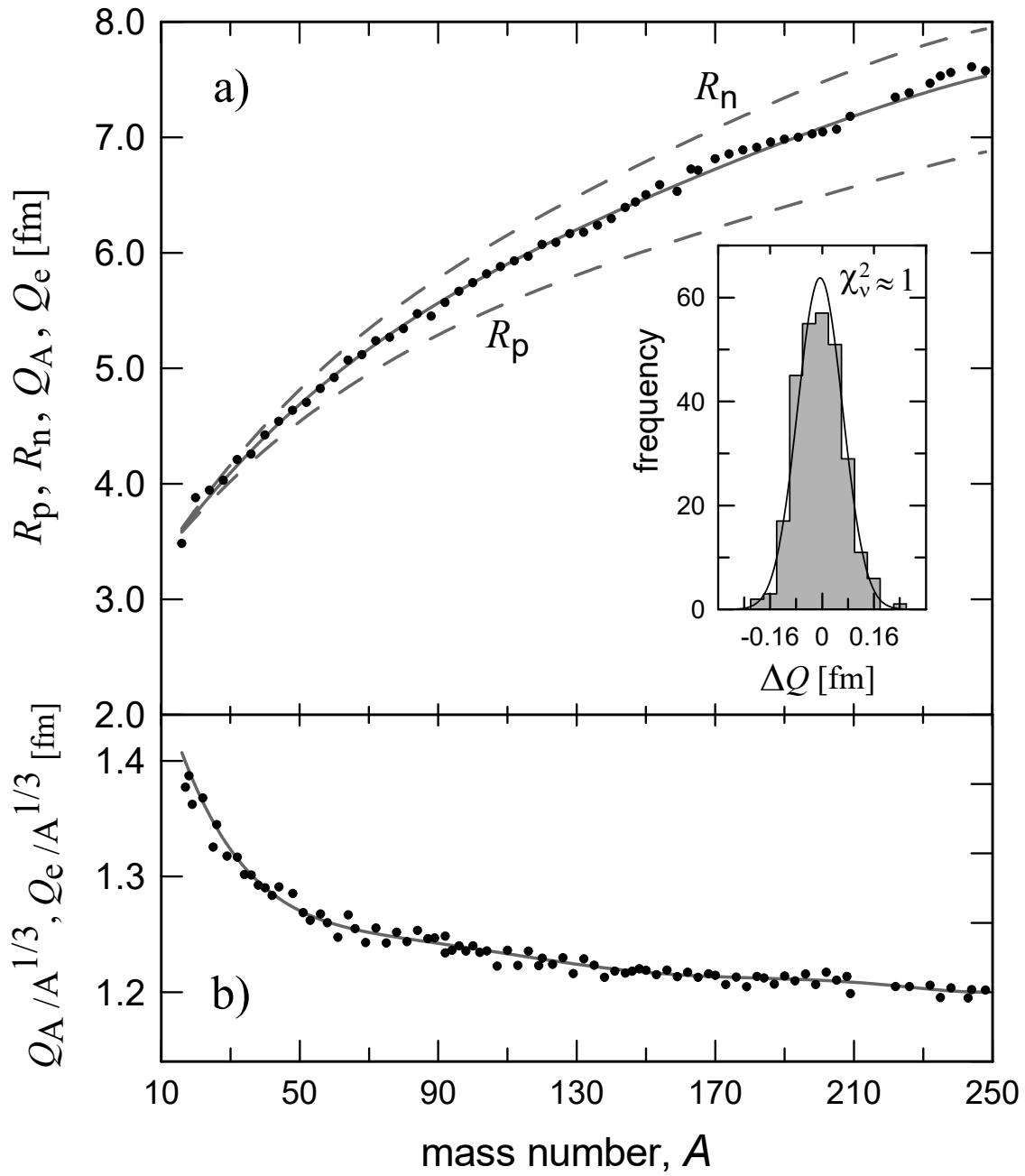


Figure 1

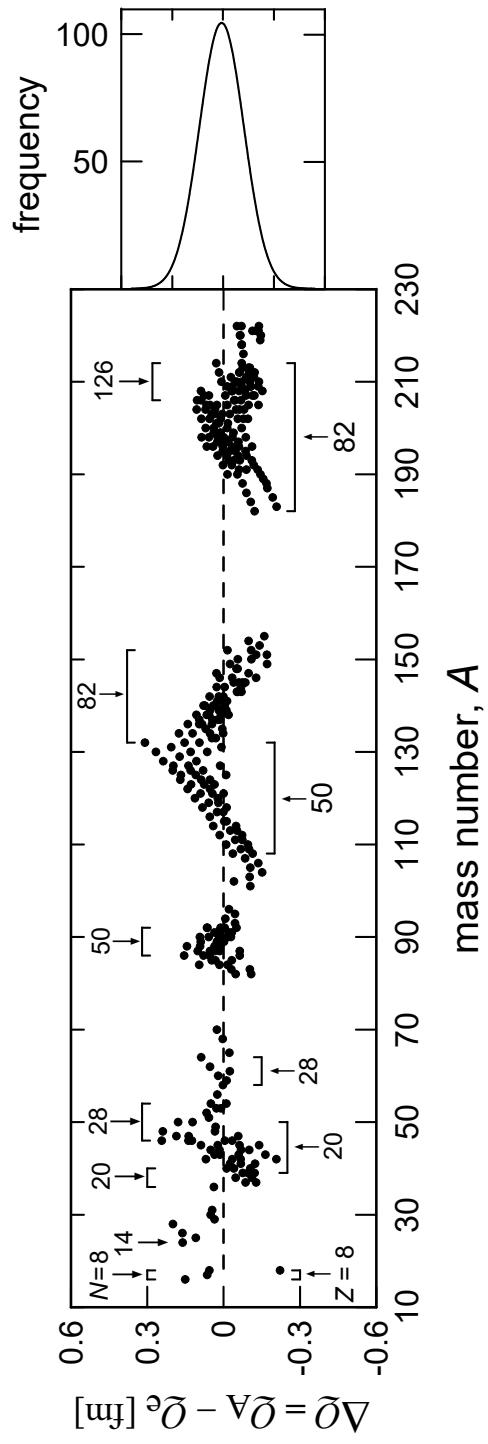


Figure 2

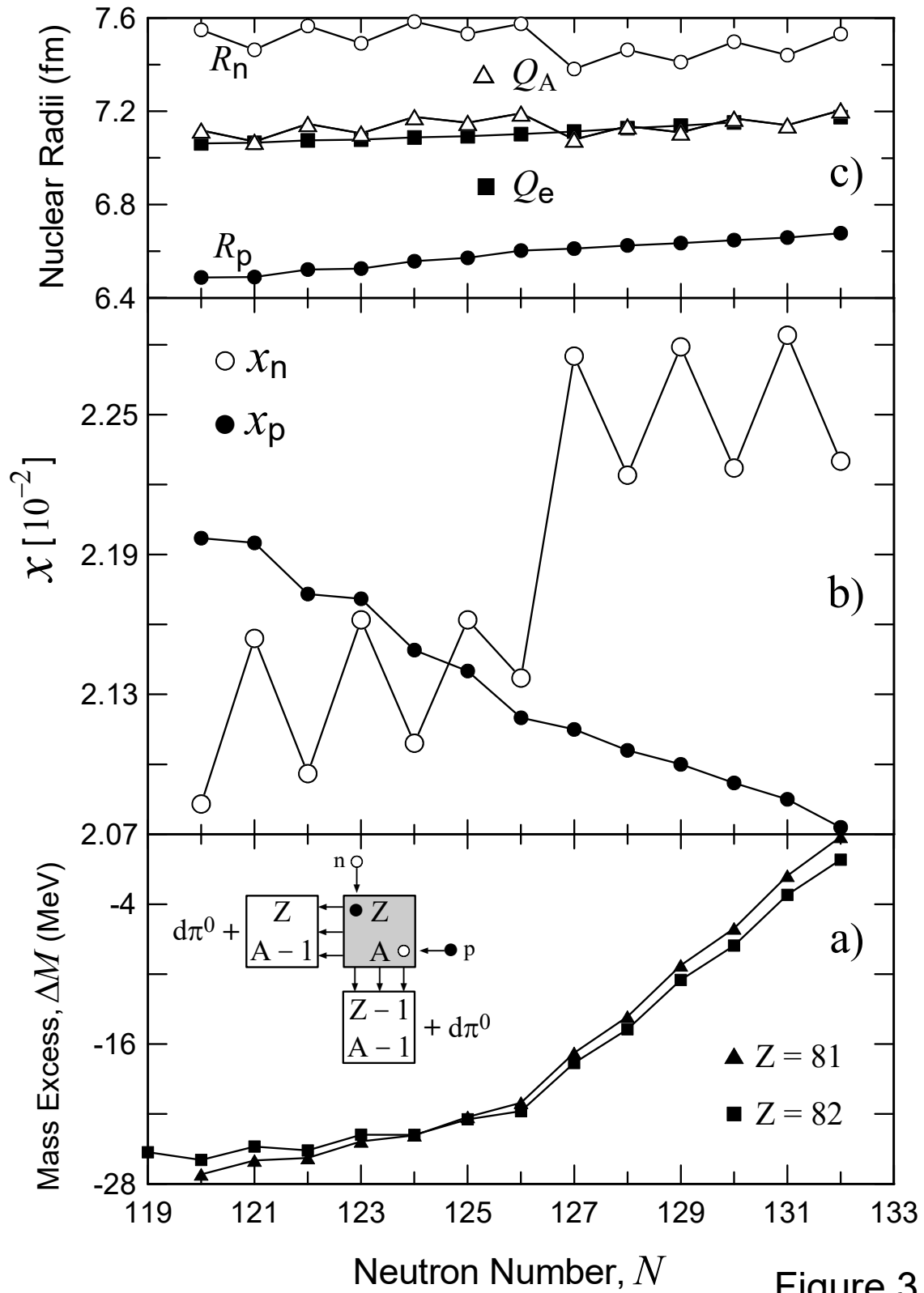


Figure 3

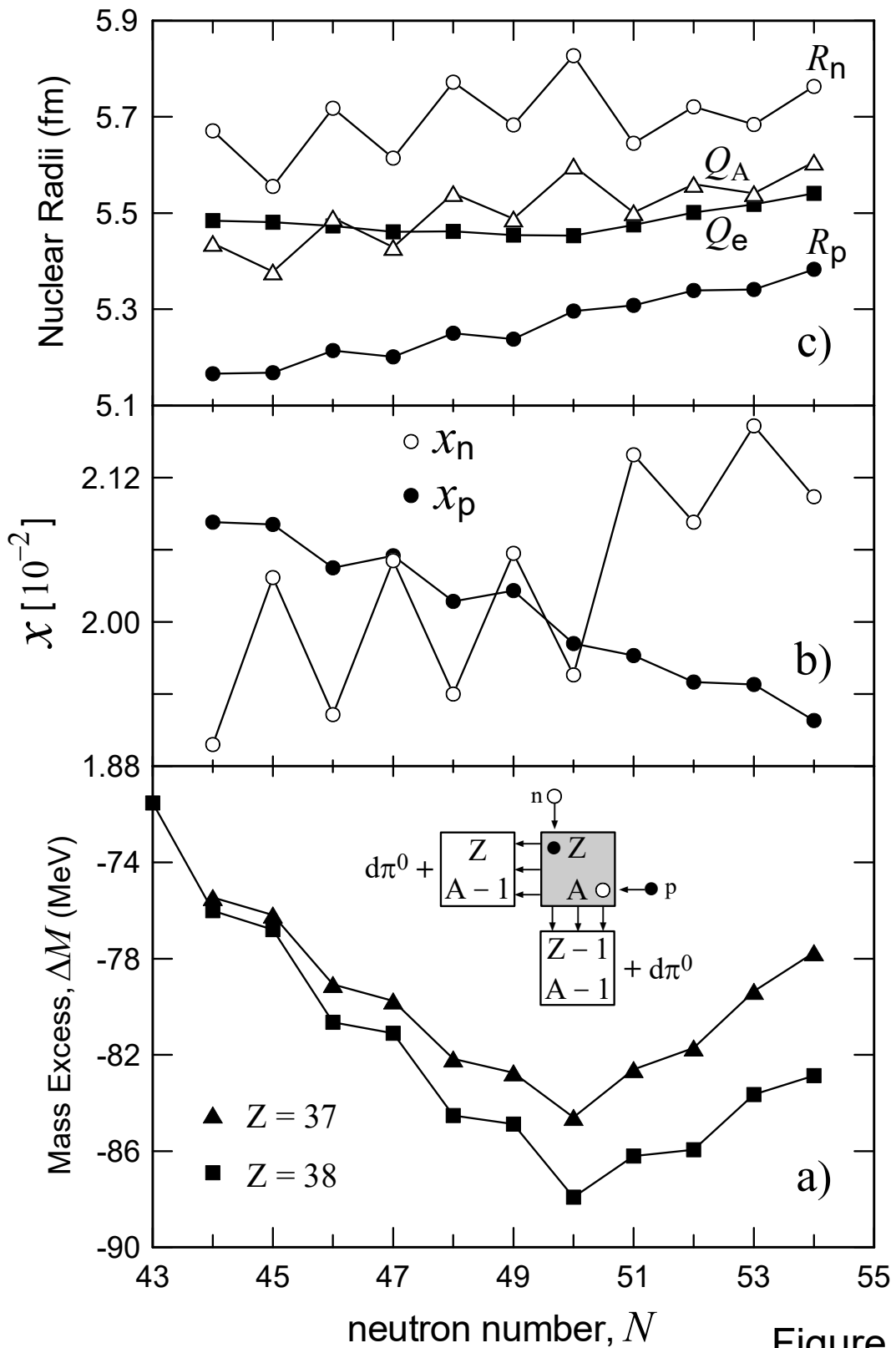


Figure 4